Hysteresis Phenomena in the NO−H_2 Reaction over Ru(0001)†

C. A. de Wolf,* M. O. Hattink, and B. E. Nieuwenhuys

Leiden Institute of Chemistry, Gorlaeus Laboratories, Leiden University, P.O. Box 9502, 2300 RA Leiden, The Netherlands

Received: October 18, 1999; In Final Form: January 11, 2000

The NO−H_2 reaction was studied at NO pressures between 7.7×10^{-8} and 7.7×10^{-7} mbar and for H_2/NO ratios varying from 6 to 127. Hysteresis phenomena were observed during a heat and cool cycle dependent on the H_2/NO ratio, with the heating branch exhibiting less activity than the cooling branch. Apart from the H_2/NO ratio, the shape of the hysteresis also depends on the heating rate and the NO pressure. An almost 100% selectivity toward N_2 is observed with only small amounts of NH_3 formation at higher H_2/NO ratios. From the AES and TDS experiments it was concluded that an O layer that is inactive to reaction with hydrogen is responsible for the low reaction rate on the heating branch. Once the O layer is removed, the total reaction rate is determined by the removal of N_{ads}. The lateral interaction between O_{ads} and N_{ads} turns out to be repulsive.

1. Introduction

With the increasing number of cars, the need for a selective and readily available automotive catalyst is obvious. Apart from the oxidation of hydrocarbons and CO, this catalyst should be able to reduce nitrogen oxides to dinitrogen. The so-called three-way catalyst combines these qualities and consists of Pt and Rh or Pd. However, these metals are scarce, and due to the presence of various gases in the outlet gas, not only are the nitrogen oxides converted into dinitrogen but also less desirable products such as NH_3 and N_2O can be formed.

It has long been recognized that ruthenium would be a far more selective catalyst for the reduction of nitrogen oxides to dinitrogen with a minimum of NH_3 production.[1−6] Unfortunately, volatile and toxic ruthenium oxides are formed under the conditions present in the automotive catalysis, which make ruthenium-based catalysts unpractical for this application.[7] Nevertheless, the high selectivity toward dinitrogen makes Ru surfaces an interesting subject for fundamental studies.

Both Rh and Pt single-crystal surfaces are known to show nonlinear behavior such as hysteresis phenomena in the rate of N_2 formation, spatiotemporal behavior and oscillations in rate of the NO−H_2 reaction.[8−10] During the oscillations not only the activity of the surface changes periodically in time but also the selectivity can change from one product to the other and vice versa. Also the (110) surface of Ir, another Pt-group metal, shows oscillatory behavior for this reaction, as is manifested by oscillations in both rate and selectivity.[11,12]

Through the analysis of this dynamic behavior, useful information about the reaction mechanism that is involved may be obtained. In the case of Rh single-crystal surfaces consisting of (111) terraces and (100), steps the selectivity changes periodically between N_2 and NH_3 in the oscillatory regime.[13−15] For Pt(100) the surface oscillates between a state producing both N_2 and NH_3 to a state for which the minor byproduct N_2O is formed with maximum rate.[16−19] Since Ru shows an almost 100% selectivity toward N_2, oscillations in the selectivity are unlikely to occur and a different origin of the nonlinear behavior might be the result.

Although a large number of studies have been dedicated to the adsorption of NO[20−27] or H_2[28−34] on Ru(0001), only a limited amount of studies have been focused on the NO−H_2[35,36] reaction. To our knowledge no report on nonlinear behavior over Ru single crystal exists for this reaction. In this article hysteresis phenomena in the NO−H_2 reaction over Ru(0001) will be described.

2. Experimental Section

The reactions were performed in a UHV system equipped with LEED, AES, and a differentially pumped (60 L/s) quadrupole mass spectrometer (MS). The system was pumped by a turbo molecular pump (150 L/s) and an ion pump (150 L/s). The base pressure was always better than 4×10^{-10} mbar.

The crystal (diameter of ca. 0.7 mm) was cut within 0.5° of the desired direction and polished down to a grain size of 0.1 μm. The crystal was spot-welded to a Ta wire and could be resistively heated to 1200 K. The temperature was measured using a Pt−Pt/Rh thermocouple spot-welded to the side of the crystal.

The crystal was cleaned by repetitive treatments with oxygen, Ar^+ ion sputtering, and flashing in vacuum. Residual oxygen was removed by annealing in hydrogen for several minutes at 700 K.

The AES measurements were performed using a single pass cylindrical mirror analyzer with an incident electron energy of 2.0 kV. To check the influence of the electron beam on the reaction, a heat and cool cycle was performed directly after the AES measurements and the MS intensities were compared with previous measurements.

During the reactions only the turbo molecular pumps were used and the crystal was turned in front of a small opening (diameter of ca. 1 mm), which gave access to the MS chamber. The distance between the QMS hole and the crystal was typically 0.2 mm. In this way the sensitivity was increased and the contributions from the Ta support filaments and the edges of the crystal were minimized. When the crystal was turned away from the QMS hole, the pressure readings of the QMS

† Part of the special issue "Gabor Somorjai Festschrift".

* Corresponding author. Tel: (31) 71 5274484. Fax: (31) 71 5274451. E-mail: c.wolf@chem.leidenuniv.nl.

10.1021/jp993716t CCC: $19.00
Published on Web 03/18/2000

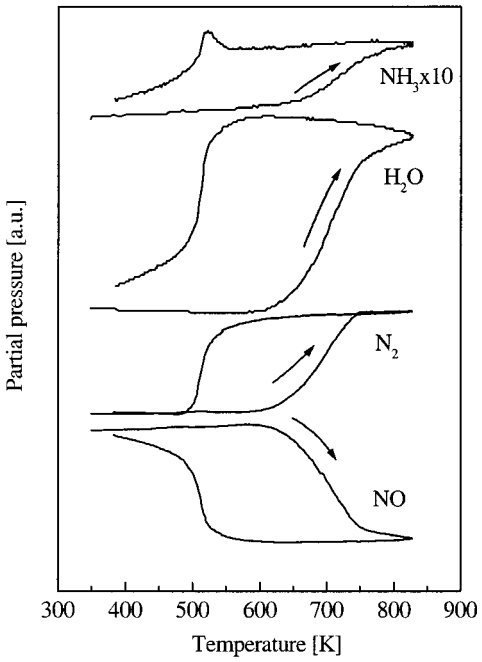

Figure 1. Rates of NO conversion and NH_3, H_2O, and N_2 formation during a heat and cool cycle at a NO pressure of 7.7×10^{-7} mbar and a H_2/NO ratio of 20. The heating rate is 0.5 K/s.

returned to the noise level, indicating that the observed phenomena are caused solely by the reaction over the crystal.

For NH_3 amu 16 was followed instead of amu 17 to avoid interference with OH, a cracking product from water. Gases of high purity (Messer Griesheim, commercial purity 99.5−99.999%) were dosed by means of two leak valves from the dosing system into the main chamber. The pressure readings of the ion gauge were corrected using relative sensitivities for NO and H_2 to N_2 of 1.3 and 0.46, respectively.

Before the heat and cool cycles were started, the NO pressure was stabilized for half an hour, and after the H_2 pressure was changed, the second cycle was recorded, which proved to be perfectly reproducible.

3. Results

The NO−H_2 reaction has been studied over a wide range of H_2/NO (R) ratios in the temperature regime from 300 to 830 K for NO pressures ranging from 7.7×10^{-8} to 7.7×10^{-7} mbar. The main reaction products were N_2 and water, and only small amounts of NH_3 were formed even in a large excess of hydrogen. No N_2O was detected for all conditions studied.

Figure 1 shows an example of a heat and cool cycle at a NO pressure of 7.7×10^{-7} mbar and $R = 20$. From this figure it is clear that a large hysteresis in the formation of N_2 and H_2O and in the consumption of NO exists, with the crystal being more active on the cooling branch than on the heating branch. Upon heating, the consumption of NO starts at 600 K, leading to the formation of N_2 and H_2O. Around 650 K a small amount of NH_3 is formed, which reaches a plateau at 800 K. For the N_2 production a plateau is reached at 750 K, while the H_2O formation does not reach a plateau on the heating branch in the temperature range examined.

On the cooling branch the maximum NO conversion is maintained without changes in the selectivity toward N_2 or NH_3 until a temperature of 550 K is reached. At this temperature the H_2O formation reaches its maximum. Upon a further decrease in temperature, the N_2 and H_2O formation start to drop, accompanied by a small increase in the NH_3 production, which is at its maximum at 520 K. At 490 K the reaction stops.

It was found that the width of the hysteresis depends strongly on the H_2/NO ratio, as is demonstrated in Figure 2. At a H_2/NO ratio of 6 the N_2 formation does not reach a plateau on the heating branch in the temperature regime studied. On the cooling branch the NO conversion and, as a consequence, the N_2 formation (at this ratio no NH_3 is formed) increase until a maximum is reached around 750 K. At temperatures lower than 520 K no reaction takes place.

Starting from a H_2/NO ratio of 13, a plateau is reached in the N_2 formation, which shifts to lower temperatures upon increasing the H_2/NO ratio. On cooling, the influence of the H_2/NO ratio on the reaction rate is much less once the plateau in the NO conversion is reached. For all the ratios the reaction stops at temperatures below 490 K after a maximum in the NH_3 production is reached at 520 K. Because of the enhanced H_2/NO ratio the selectivity toward NH_3 increases, leading to a less drastic drop in the N_2 formation on the cooling branch. At a ratio of 65 (not shown) the heating and cooling branch collide.

The hysteresis phenomena depend not only on the H_2/NO ratio but also on the NO pressure. For example, at a NO pressure of 1.5×10^{-7} mbar no plateau is reached for the N_2 formation at a ratio of 14, while for NO pressures higher than 3.8×10^{-7} mbar a plateau is observed already for a ratio of 13. However, at $p(NO) = 7.7 \times 10^{-8}$ mbar the heating and cooling branch collide at a H_2/NO ratio of 20, while for a 10 times higher NO pressure a ratio of 65 is needed for the hysteresis to disappear.

Another remarkable feature is the influence of the heating rate on the formation of N_2 and H_2O at low NO pressures, as is illustrated in Figure 3. At a heating and cooling rate of 0.1 K/s a low-temperature feature at 480 K is observed for N_2 on the heating branch, followed by an increase in the reaction rate at 550 K. Apart from the low-temperature feature, the rate of H_2O formation is comparable with the rate of N_2 formation. A plateau in the N_2 formation is reached at 690 K. Starting with a heating rate of 0.5 K/s, new features in both the N_2 and the H_2O formation are observed. The N_2 formation starts with a very sharp peak with a maximum at 490 K followed by a smaller feature at 560 K. The H_2O formation shows a maximum at 520 K that is accompanied by a local minimum in the N_2 formation. When the heating rate is further increased, these features get more pronounced and the high-temperature maximum in the N_2 formation shifts to higher temperatures. However, the cooling rate has hardly any effect on the reaction rate. At NO pressures higher than 7.7×10^{-8} mbar, the heating rate has no influence on the reaction rate.

To get a better insight into the processes that are responsible for the observed hysteresis phenomena, knowledge of the species present on the surface during the reaction is needed. One way to obtain this information is by following the reaction with AES. Unfortunately, the use of the AES equipment only allows for NO pressures lower than 1×10^{-7} mbar, but since the main features are comparable for all the NO pressures used, these measurements can still provide valuable information. In Figure 4 the AES results of the heat and cool cycle with a NO pressure of 7.7×10^{-8} mbar and an H_2/NO ratio of 20 are shown. The N_{381} and O_{510} peak to peak heights were measured and normalized against the Ru_{231} peak to exclude the influence of a fluctuating electron beam. Figure 4 shows clearly that both the N_{381} and the O_{510} signal exhibit a large hysteresis in the temperature window between 450 and 650 K. However, the hysteresis in the N_{381} signal is counterclockwise while for O_{510} it is clockwise.

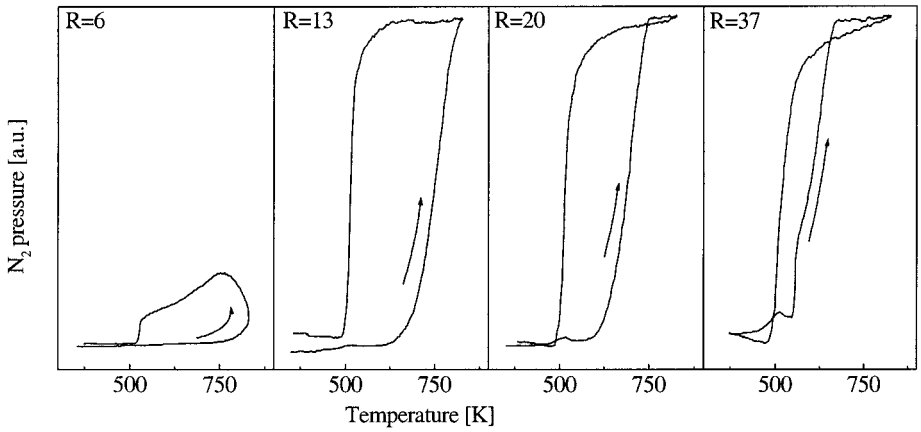

Figure 2. Rate of N_2 formation during a heat and cool cycle at a NO pressure of 7.7×10^{-7} mbar and H_2/NO ratios of 6, 13, 20, and 37, respectively. The heating rate was 0.5 K/s.

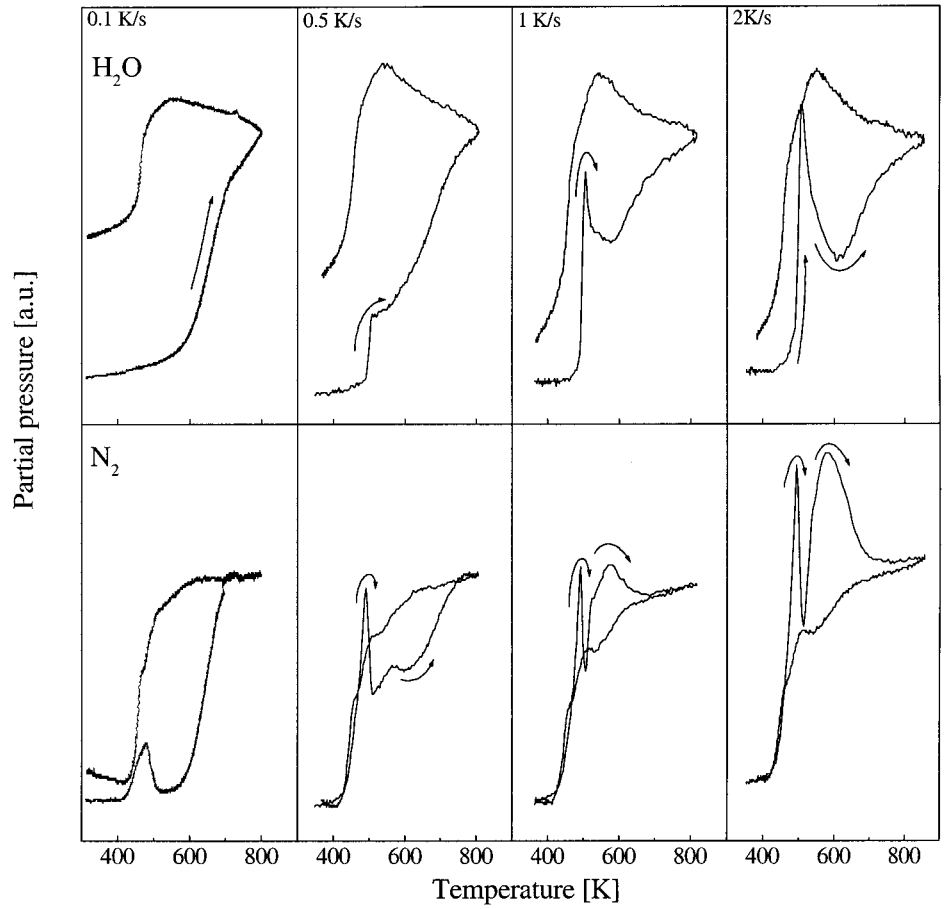

Figure 3. Rates of N_2 and H_2O formation during a heat and cool cycle at a NO pressure of 7.7×10^{-8} mbar and a H_2/NO ratio of 20. The heating rate was 0.1, 0.5, 1, and 2 K/s, respectively.

At room temperature a N_{381} signal is measured in addition to a small O_{510} signal. Upon an increase in temperature, the N_{381} signal decreases in addition to an increase in the O_{510} signal. The N_{ads} leaves the surface as N_2 in the temperature regime between 425 and 500 K. After the N_2 desorption only a O_{510} signal is observed followed by the formation of water at a temperature of 625 K. Remarkably, the O_{510} peak does not completely disappear even at temperatures as high as 830 K. On cooling, a further increase in the water formation rate is observed and the O_{510} peak disappears between 660 and 550 K. At the same time the N_{381} signal increases and reaches a maximum at 500 K. At this temperature the N_{381} signal drops and the O_{510} peak increases dramatically. The surface returns to its original coverage upon further cooling.

In addition to knowledge of the surface coverage during the reaction, information about the interaction between the different species is necessary. To obtain some of this information, the following experiment was carried out. First, NO was dosed onto a clean surface at room temperature. After evacuation of the NO, hydrogen was introduced and a TDS-like experiment was carried out. To exclude a contribution from residual CO, mass 14 was also recorded, which proved to be a combination of the N_2 and NO signal. In Figure 5 the results of this experiment are compared to a TDS experiment in the absence of a flow of hydrogen. We would like to stress that these data are merely meant to qualitatively compare the data obtained with and without a flow of hydrogen and should not be used for quantitative interpretations. It can be seen from Figure 5B that

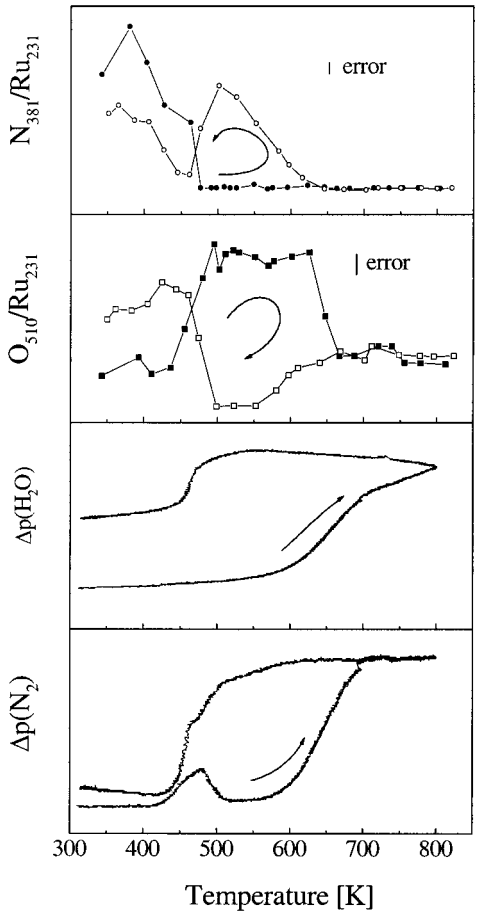

Figure 4. N_{381}/Ru_{231} and O_{510}/Ru_{231} AES signal ratios in addition to the N_2 and H_2O formation rates at a NO pressure of 7.7×10^{-8} mbar and a H_2/NO ratio of 20. The solid symbols represent the heating branch, and the open symbols represent the cooling branch.

two NO peaks are observed, in the literature called $\nu 1$ and $\nu 2$ and that several N_2 peaks exist, the one at 467 K being the most pronounced.[22] Feulner et al. discriminated three N_2 peaks labeled $\beta 1$ to $\beta 3$.[23] No N_2O desorbed from the surface under the conditions used, probably because of the high adsorption temperature. As can be seen from Figure 5A, the introduction of H_2 into the flow has no influence on the NO desorption states. However, in the N_2 desorption spectrum some changes can be observed. The first desorption maximum is still at 467 K, but at higher temperatures a new feature is observed between 550 and 900 K. Between the low-temperature desorption state of N_2 and this high-temperature feature, water is desorbing with a very sharp leading edge. Hardly any NH_3 is formed under the conditions used.

Because of the large amounts of oxygen present on the surface on the heating branch of a heat and cool cycle, information about the interaction between NO and O_{ads} will be essential to elucidate the mechanism responsible for the hysteresis phenomena. Therefore, an increasing amount of O_2, which dissociates into O_{ads} at temperatures higher than 80 K,[37] was dosed onto a clean surface at room temperature followed by a constant dose of NO. The amount of NO was low enough for complete dissociation on a clean Ru(0001) surface. From Figure 6 it can be seen that, upon an increase in the dose of oxygen, NO starts to desorb in one single state. The N_2 desorption states shift to a much lower temperature upon adsorption of the slightest amount of oxygen and the high-temperature shoulder starts to diminish, resulting in a decrease of the total integrated intensity of the N_2 peaks. From an O_2 dose of 2.3 Langmuir the amounts of N_2 and NO desorbing from the surface do not decrease anymore with increasing O_2 exposure. No NO_2 or N_2O was observed under these conditions.

Since the existence of some features in the temperature hysteresis over rhodium are thought to be related to oscillatory behavior, several attempts were made to obtain macroscopic rate oscillations over Ru(0001).[15] However, oscillations were not observed either by scanning slowly through the temperature regime at different NO pressures and for several H_2/NO ratios or by varying the H_2 pressure at constant temperature.[8−18]

4. Discussion

To construct a model that describes the hysteresis phenomena in the NO−H_2 reaction over Ru(0001), knowledge about the elementary steps involved is necessary. The following reaction steps need to be considered:

$$NO + \# \leftrightarrow NO_{ads} \quad (1)$$

$$H_2 + 2\# \leftrightarrow 2H_{ads} \quad (2)$$

$$NO_{ads} + \# \rightarrow N_{ads} + O_{ads} \quad (3)$$

$$2N_{ads} \rightarrow N_2 + 2\# \quad (4)$$

$$O_{ads} + 2H_{ads} \rightarrow H_2O + 3\# \quad (5)$$

$$N_{ads} + 3H_{ads} \leftrightarrow NH_{3,ads} + 3\# \quad (6)$$

$$NH_{3,ads} \rightarrow NH_3 + \# \quad (7)$$

where # denotes a vacancy.

Since the NO and H_2 adsorption is the subject of numerous studies, a lot of information is available concerning reaction steps 1−4 that will be summarized first.

Hydrogen adsorbs dissociatively on Ru(0001), showing two desorption maxima at 325 and 380 K.[28] The origin of these two peaks has been assigned to occupation of the hcp and fcc types of 3-fold sites,[28] the distribution of H over surface and subsurface sites,[29,30] lateral interactions between H atoms adsorbed in the same kind of sites [31] and modifications in the H−Ru interlayer distance.[33] On the basis of mathematical calculations it was concluded that the surface 3-fold hollow sites and the subsurface octahedral site are the most likely adsorption sites.[32,34]

Inspired by the promising catalytic activity of ruthenium-based catalysts, researchers paid a lot of attention to the NO/Ru(0001) system in the late seventies.[20−23] NO was found to adsorb in two molecular states, labeled $\nu 1$ and $\nu 2$. With XPS[22] and EELS[20,21] the $\nu 1$ state was assigned to bridge bonded NO while the $\nu 2$ state was attributed to a linear species in an on-top position. The two peaks arising in the TDS of NO adsorbed on Ru were assigned to the two molecular states, $\nu 1$ and $\nu 2$.[23]

More recent studies with HREELS[25] and IRAS[24] showed that the NO/Ru(0001) system is a bit more complicated. In addition to the two molecular NO states $\nu 1$ and $\nu 2$, two other molecular NO states were reported: a hyponitrite form that is only present at low temperatures and low coverages and a $\nu 0$ state that is assigned to a 3-fold bridge species, the $\nu 1$ being connected with the 2-fold bridge bonded NO. The presence of the various NO states depends strongly on the temperature and the coverage. For example, at 115 K and a low coverage of NO only the $\nu 0$ state is filled, which is stable up to 350 K, the N_2 desorbing around 550 K in a second-order process. At medium coverages the $\nu 0$ behaves as described above and the NO adsorbed in the

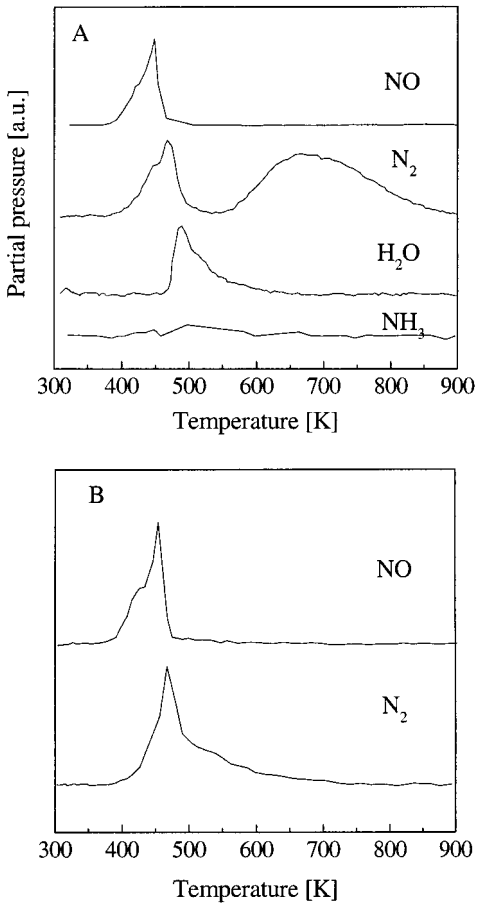

Figure 5. TD spectra of NO ($m/e = 30$), N_2 ($m/e = 28$), H_2O ($m/e = 18$), and NH_3 ($m/e = 16$) after dosing 1.16 Langmuir of NO at 300 K with (A) or without (B) 2×10^{-6} mbar hydrogen in the flow during the heating. The adsorption temperature was 300 K and the heating rate was 2 K/s.

$\nu 1$ state is transformed into the $\nu 2$ state, which partly dissociates and desorbs as N_2 in a seemingly first-order process around 450 K. At high coverages NO adsorbs in the $\nu 1$ and $\nu 2$ state from which part of the $\nu 1$ state is transformed into the $\nu 2$ state at room temperature. At higher temperatures part of the $\nu 1$ and $\nu 2$ states desorb, the other parts dissociate, giving rise to the second and first desorption maxima in the N_2 desorption spectrum. It was concluded that the dissociation is mainly connected to the $\nu 0$ and $\nu 2$ states. To add more proof to their conclusions, the authors studied the coadsorption of NO and O_2. It appeared that on an O-covered surface only the $\nu 1$(O) state is populated directly from the gas phase because O_{ads} occupies preferentially the 3-fold sites, thus blocking the $\nu 0$ state. Upon thermal activation the $\nu 1$(O) state is completely transformed into the $\nu 2$ state, producing a $\nu 2$ desorption maximum in addition to the first-order N_2 desorption peak identical to the clean surface. According to these authors, saturation of the $\nu 2$ state blocks further adsorption into the $\nu 1$(O) state.[25] A more recent study associates the site blocking with the presence of O_{ads}.[26] No second-order N_2 desorption peaks were observed, in agreement with the absence of the $\nu 0$ state.[24,26] These observations confirm the assumption that mainly $\nu 0$ and $\nu 2$ are capable of dissociating.

The TD spectra shown in Figure 5B qualitatively agree with the results of previous studies.[23,24,26] Only the relative contributions of the $\nu 1$ and $\nu 2$ NO desorption peaks are reversed, probably caused by the much lower adsorption temperature (<150 K) used in the previous studies, possibly in combination with the presence of some residual O_{ads} (below the detection limit of AES) in the 3-fold hollow sites before dosing. This was not further checked. Interference of trace amounts of CO can be excluded because CO preferentially adsorbs on on-top sites, which would block the $\nu 2$ state instead of the $\nu 1$ state.[38]

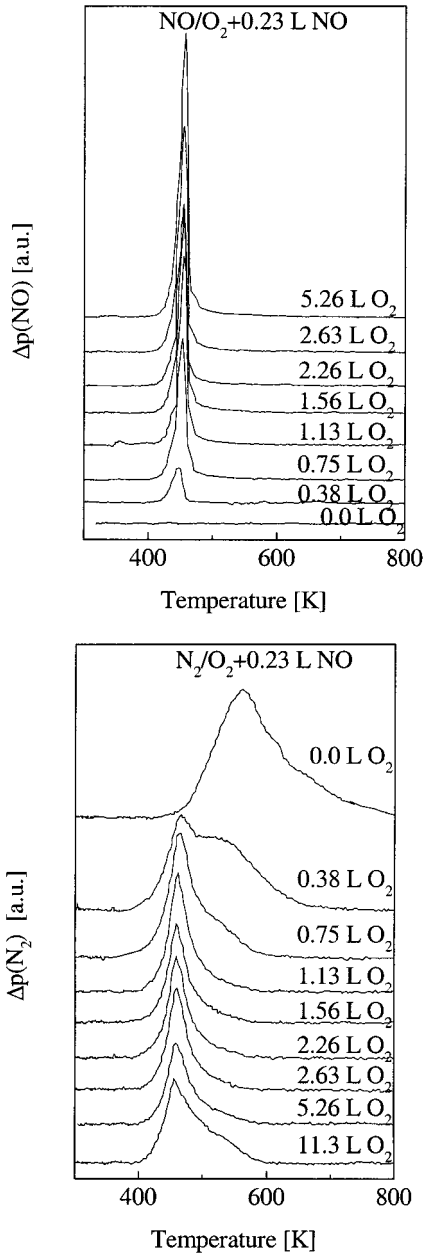

Figure 6. TD spectra of NO ($m/e = 30$) and N_2 ($m/e = 28$) from 0.23 Langmuir of NO after predosing increasing amounts of oxygen at 300 K. The adsorption temperature was 300 K, and the heating rate was 2 K/s.

From Figure 6 it can be seen that a dose of 0.23 Langmuir of NO, which corresponds to 0.26 monolayer, completely dissociates when dosed onto a clean surface at room temperature. When the predose of oxygen is increased to 2.3 Langmuir the amount of NO that dissociates is reduced to 30%. Upon adsorption of O_{ads}, NO starts to desorb in a single state corresponding to the $\nu 2$ state in the TD spectra of NO from a clean surface at higher coverages. This observation corresponds to previous studies on the O/NO/Ru(0001) system for higher NO coverages[24−26] and can be explained as follows: at room-temperature all the $\nu 1$(O) is converted into the $\nu 2$ state, giving rise to a sharp $\nu 2$-desorption peak and the seemingly first-order N_2 desorption maximum upon heating. These results confirm

the conclusions by Conrad et al. [25] that dissociation is connected to the $\nu 2$ state. Only at low O_{ads} coverages can a small amount of NO still adsorb in the $\nu 0$ state, leading to the second-order desorption maxima in the N_2 desorption spectrum.

When the predose of oxygen is increased, dissociation becomes suppressed because O_{ads} blocks the sites for the dissociation products. This leads to the saturation of the $\nu 2$ state, which might prevent further adsorption from the gas phase into the $\nu 1$(O) state.[25] From our results we cannot exclude that site blocking by O_{ads} causes the sticking coefficient of NO to drop to zero.[26] As a consequence, the total amount of NO adsorbing on the O layer reaches a constant value as ≥ 2.3 Langmuir of O_2 is predosed.

Now we can start the examination of the NO−H_2 reaction by looking at the TDS results of Figure 5. It is clear that no changes in the desorption states of NO occur by the introduction of H_2. After desorption of NO, N_2 starts to desorb in the same way as in the spectrum shown in Figure 5B, which is to be expected since this maximum shows a first-order behavior connected to the desorption of the $\nu 2$ state of NO. At higher temperatures, H_2O desorbs at a constant temperature for all the NO coverages ≥ 0.32 Langmuir indicative of first-order kinetics. However, at lower coverages, the H_2O desorption shifts to lower temperatures. Looking at the form of these H_2O desorption peaks and considering the fact that the desorption maximum shifts only to a lower temperature for coverages of NO that show no desorption maximum assigned to the $\nu 2$ state, it is likely that the desorption of this H_2O is connected to the desorption of N_2. Since the NO is already partly dissociated at room-temperature, H_2O formation was expected at lower temperatures, as happened for coverages lower than 0.32 Langmuir of NO. Apparently, either NO_{ads} or N_{ads} is blocking the adsorption of H_2. According to Thiel et al.,[35] H_2 adsorption is not blocked by the presence of an NO layer of 55 Torr s on the surface, besides NO in the 3-fold hollow site is not stable at temperatures higher than room temperature, as mentioned before. This suggests that the H_2 adsorption is blocked by the N_{ads} on the surface, which also occupies the 3-fold hollow sites. This is in agreement with the results of Seets et al.,[39] who concluded that no H_2 can adsorb on a surface covered with 0.33 monolayer of N_{ads} at temperatures higher than 320 K. In addition, according to Koch et al.[40] O_{ads} can also influence the sticking probability of H_2 dependent on the coverage. At 0.25 monolayer $< \theta_O <$ 0.50 monolayer, a reactive O(2 × 1) layer is formed after adsorption of O_2, while for θ_O close to 0.50 monolayer, a vanishing sticking probability of H_2 was observed. However, in this experiment a coverage of 0.5 monolayer of O_{ads} is never reached, because part of the NO always desorbs molecularly.

Increasing the temperature further leads to a second N_2 desorption maximum. This is connected with the second-order maximum in Figure 5B, which is now shifted to higher temperatures in the absence of O_{ads}, indicating that the lateral interactions between O_{ads} and N_{ads} are repulsive. The absence of NH_3 production shows that either reaction 4 is favored over reaction 5 under our conditions or the production of N_2 proceeds through the formation of NH_x, as has been suggested for supported Ru catalysts,[4,5] although other studies conclude that this is not the major pathway for the N_2 formation.[1,2] The high selectivity for N_2 was explained by the high N_{ads} surface coverage.[6] Moreover, Nishida et al.[36] did not observe an NH_x species with UPS or XPS during the NO−H_2 reaction over Ru(0001) (although it is questionable whether these techniques are sensitive enough to discriminate between N_{ads} and $NH_{x,ads}$) and Thiel et al.[35] did not mention species other than NO_{ads}, N_{ads}, and O_{ads} after studying the coadsorption of NO and H_2 over a Ru(0001) single-crystal surface with EELS. Using only TDS, we cannot exclude the formation of NH_x as an intermediate in the N_2 production, although it would be highly coincidental that the second-order N_2 desorption peak in the TDS experiment of Figure 6A shows exactly the same behavior as the second-order N_2 desorption peak after a low coverage of NO under normal TDS conditions.

The next step necessary to understand the mechanism of the hysteresis phenomena is the examination of the species present on the surface during the reaction. Unfortunately, by using AES, we cannot discriminate between NO_{ads}, $NH_{x,ads}$, and N_{ads}. The O_{510} signal can be assigned to O_{ads} because NO_{ads} is not visible at this energy due to shielding. From Figure 4 it appears that at room temperature the surface is covered with a N species and small amounts of O_{ads}. Using the HREELS[25] results, we can assign this N species to molecular NO and atomic N_{ads}. Upon an increase in temperature, the N_{381} signal starts to decrease, indicating that NO desorbs or dissociates and that reaction 4 takes place, leading to a maximum in the N_2 formation, which is not connected to the NO−H_2 reaction but is caused by the dissociation of NO, comparable to the low-temperature N_2 desorption maximum in the TDS experiment shown in Figure 5. As a result of the dissociation of NO, the amount of O_{ads} on the surface is increasing until a plateau is reached between 475 and 625 K. Because of the presence of the O layer, further reaction is blocked, indicating that O_{ads} is responsible for the site blocking of NO[26] rather than the saturated $\nu 2$ state of NO,[25] because under these conditions no molecular NO is present. Interestingly, this O layer is not removed by the hydrogen, which implies that reaction 5 cannot take place under these conditions since molecular H_2O would desorb at temperatures below room temperature.[41] In agreement with our LEED observations, we conclude that the surface is covered with a saturated O(2 × 1) layer, which reduces the sticking probability of hydrogen to zero.[40] Shi et al. described this low reaction rate as an induction time.[42] After this induction time the reaction rate increases and the O layer reacts to form gaseous H_2O. The change in the reaction rate can be explained by the existence of some inactive O(2 × 2) islands that can adsorb and dissociate H_2, which is followed by the reaction between H_{ads} and O_{ads} on the boundaries of the active O(2 × 1) islands. Once an O_{ads} at the rim of an O(2 × 1) island is reacted away, an inactive O(2 × 2) superstructure is formed. Eventually, this process leads to a surface covered with a saturated O(2 × 2) layer, which is completely inactive to the formation of H_2O under the conditions used by Koch et al.[40]

In the case of Figure 4 this means that the amount of O_{ads} in excess of 0.25 monolayer, the so-called active oxygen,[42] is reacted away quickly. However, the less active oxygen ($<$0.25 monolayer) does not react to form H_2O, probably because the hydrogen equilibrium coverage becomes increasingly reduced by recombinative desorption or by a temperature-dependent sticking coefficient of H_2.[40] As a consequence, a constant coverage of 0.25 monolayer of O_{ads} is present on the surface due to the steady supply of O_{ads} through the dissociation of NO. Since the increase in the H_2O formation is accompanied by an increase in the N_2 production, the residual O layer does not completely block the dissociation of NO, which is in agreement with our TDS results.

Upon cooling, the surface remains covered with 0.25 monolayer of oxygen until reaction 5 can take place again, leading to the removal of all the O_{ads} in addition to the increase in the N_{381} signal, which can be assigned to atomic N because no NH_3

is formed under these conditions. Since this increase in the H_2O formation was also observed in the O_2-H_2 reaction, we exclude the possibility that the decrease in the O_{510} signal is a consequence of the increase in the N_{381} signal. The buildup of N_{ads} can be explained by the repulsive interactions between O_{ads} and N_{ads}. In the absence of O_{ads}, N_{ads} is no longer pushed away from the surface and the amount of N_{ads} will therefore increase for temperatures below the desorption temperature of N_2 from an oxygen free surface (see Figure 6). As a consequence the N_2 formation decreases slightly. At a temperature of approximately 500 K the reaction rate of reaction 5 is reduced to zero, as is concluded from the O_2-H_2 experiments, and an O layer is built up again. This is in agreement with Li et al. who concluded that the crystal temperature is critical for the reaction of D_2 with O_2 irrespective of the D_2/O_2 ratio.[43] Due to repulsive interactions between O_{ads} and N_{ads}, the nitrogen atoms react to form gaseous N_2. At lower temperatures, the N_{381} signal increases again due to the adsorption of NO, which cannot completely dissociate on an O-covered surface, as is concluded from Figure 6.

Now we can easily understand the influence of the NO pressure, the H_2/NO ratio, and the heating rate on the hysteresis phenomena. Increasing the NO pressure at a constant H_2/NO ratio leads to an increase in the width of the hysteresis, which is caused by the shift of the heating branch to higher temperatures. This can be explained by the increased equilibrium oxygen coverage at higher NO pressures, which prevents the dissociative hydrogen adsorption, thus blocking further reaction until higher temperatures are reached. Once the hydrogen has gained access to the surface and the reaction between O_{ads} and H_{ads} has reached a steady state, NH_3 is also formed, as can be seen in Figure 1. A higher NO pressure at constant H_2/NO ratio will result in higher N_{ads} and H_{ads} coverages and, hence, in a higher rate of NH_3 formation. On the cooling branch, the NH_3 production decreases slightly because reaction 5 is favored over reactions 6 and 7. Around 500 K the H_2O formation rate is reduced and a maximum in the NH_3 signal is observed instead of an increase in the N_2 formation, as was observed for lower NO pressure (see Figure 4).

Increasing the H_2/NO ratio at a constant NO pressure reduces the hysteresis, as shown in Figure 2, because less oxygen remains on the surface after a complete heat and cool cycle is finished and this oxygen is more easily removed due to the higher equilibrium coverage of hydrogen. In addition, the selectivity toward NH_3 increases, causing the decline in the N_2 formation of the cooling branch at higher H_2/NO ratios.

Figure 2 also shows that the maximum N_2 formation rate is independent of the hydrogen pressure under conditions where a plateau is reached in the N_2 formation. This is in agreement with the observations by Nishida et al.[36] for an oxygen-free Ru(0001) surface and was explained by the desorption of N_{ads} being the rate-determining step.

The influence of the heating rate on the hysteresis phenomena at an NO pressure of 7.7×10^{-8} mbar can be explained by looking at the comparison between Figure 5 and Figure 3. The very sharp TDS-like peak in the N_2 production during the hysteresis at heating rates ≥ 0.5 K/s is followed by a sharp peak in the water formation that is comparable to the one in Figure 5A. This suggests that the oxygen that remains on the surface after the removal of N_{ads} does not block the dissociative adsorption of hydrogen, probably because the NO adsorption or dissociation is not fast enough to reach the critical 0.5 monolayer of O coverage at heating rates ≥ 0.5 K/s. Once the oxygen is removed, the second-order N_2 desorption peak, comparable to the high-temperature peak in Figure 5A, is observed in addition to the N_2 formed from dissociation of NO adsorbed on the (partly) O-free surface. The N_2 formation is less influenced by the cooling rate, because now no O layer is present and the reaction rate is determined by the desorption of N_{ads}.

To propose a mechanism for the hysteresis over Ru(0001), it is useful to compare the observed phenomena with the nonlinear behavior over other Pt-group metals. For the nonlinear behavior in the $NO-H_2$ reaction over Pt(100) two mechanisms have been proposed.[16−19] In the first model a transition between the hex and the (1×1) phase was used to explain the hysteresis phenomena. The (1×1) phase, which is very active in the dissociation of NO, is formed due to the high coverage of NO at low temperatures, leading to the formation of N_2. Upon an increase in temperature, the NO surface coverage drops below a critical value and the surface reconstructs to the inactive hex phase. On the cooling branch, the NO surface coverage increases once the temperature is low enough, and the reaction rate is restored again once the reconstruction is lifted.[18,19] Since the oscillations have been observed in the same temperature regime as the occurrence of the hex $\rightarrow 1 \times 1$ transition, the oscillations were considered to be related to this phase transition.[19] However, Cobden et al. concluded that the reconstruction may not play a crucial part in the oscillatory cycle.[17] Instead, they proposed a mechanism in which the presence of vacancies for the dissociation of NO determines the rate of N_2 formation. At first, the surface is covered with NO and the dissociation of NO is inhibited due the lack of vacancies. Once some of the NO is desorbed, vacancies are created, leading to the autocatalytic formation of N_2, known as a surface explosion. Because of the buildup of oxygen, the NO dissociation becomes inhibited again, and with the consequent buildup of NO, the oscillatory cycle is back at the initial situation.

For rhodium surfaces consisting of (111) terraces and (100) steps[13−15] and for Ir(110)[11,12] a mechanism was proposed in which the surface oscillates between an O_{ads}-rich layer and a N_{ads}- or $NH_{x,ads}$-covered surface. The repulsive interactions between O_{ads} and N_{ads} are considered to be the driving force behind the oscillations. By following the species present on the Ir(110) surface during the heat and cool cycle with fast XPS, it was discovered that a N_{ads} layer is built up during the formation of NH_3 and H_2O, which eventually blocks the dissociative adsorption of H_2 followed by a change in the selectivity from NH_3 to N_2.[44] In the oscillatory cycle, the selectivity changes back to NH_3 once the N_{ads} layer has left the surface as N_2 as a consequence of the repulsive interactions between N_{ads} and the O_{ads} layer that was built up in the absence of H_{ads}.

Over Ru(0001), no reconstruction, surface explosion, or buildup of N_{ads} was observed. Instead, poisoning of the surface by an O layer seems to be the most likely explanation for the observed hysteresis phenomena.

5. Conclusions

Hysteresis phenomena were observed in the $NO-H_2$ reaction over Ru(0001). On the heating branch the surface is covered with an O layer that prevents the adsorption of NO and H_2, thus blocking further reaction. At higher temperatures the active oxygen can be removed by hydrogen and $N_{ads} + N_{ads} \rightarrow N_2$ (g) determines the overall rate of the reaction. On the cooling branch the residual oxygen is completely removed and a plateau in the N_2 formation is maintained until the temperature drops below 500 K, where no H_2O formation takes place and the surface becomes poisoned by an O layer again. Depending on the H_2/

NO ratio, NH_3 is formed at the low-temperature site of the maximum in the H_2O formation.

The shape of the hysteresis depends strongly on the H_2/NO ratio, the NO pressure, and the heating rate.

From the TDS measurements we can conclude that oxygen only partly blocks the dissociation of NO, but it can prevent further NO adsorption from the gas phase if the O coverage is high enough. Moreover, the NO TDS results in a flow of H_2 show that the lateral interactions between O_{ads} and N_{ads} are repulsive.

Up until now, no oscillations were obtained over the Ru(0001) surface for the $NO-H_2$ reaction.

Acknowledgment. NWO is gratefully acknowledged for financial support. This work has been performed under the auspices of NIOK, The Netherlands Institute for Catalysis, lab. report no. UL99-2-09.

References and Notes

(1) Voorhoeve, R. J. H.; Trimble, L. E. *J. Catal*. **1975**, *38*, 80.
(2) Taylor, K. C.; Klimmisch, R. C. *J. Catal*. **1973**, *33*, 478.
(3) Kobelinski, T. P.; Taylor, B. W *J. Catal*. **1974**, *30*, 376.
(4) Davydov, A. A.; Bell, A. T. *J. Catal* **1977**, *49*, 345.
(5) Uchida, M.; Bell, A. T. *J. Catal*. **1979**, *60*, 204.
(6) Hornung, A. *Catal. Lett*. **1998**, *53*, 77.
(7) Bell, W. E.; Tagami, M. *J. Phys. Chem*. **1963**, *67*, 2434.
(8) Janssen, N. M. H.; Cobden, P. D.; Nieuwenhuys, B. E. *J. Phys.: Condens. Matter* **1997**, *9*, 1889.
(9) Imbihl, R.; Ertl, G. *Chem. Rev*. **1995**, *95*, 697.
(10) Cobden, P. D.; De Wolf, C. A.; Smirnov, M. Yu.; Makeev, A.; Nieuwenhuys, B. E. *J. Mol. Catal.*, in press.
(11) De Wolf, C. A.; Nieuwenhuys, B. E.; Sashara, A.; Tanaka, K.; Slinko, M. M.; Smirnov, M. Yu. *Surf. Sci*. **1998**, *411*, L904.
(12) De Wolf, C. A.; Nieuwenhuys, B. E.; Slinko, M. M.; Smirnov, M. Yu. *Surf. Sci*. **1999**, *433*−*435*, 63.
(13) Janssen, N. M. H.; Cobden, P. D.; Nieuwenhuys, B. E.; Ikai, M.; Mukai, K.; Tanaka, K. *Catal. Lett*. **1995**, *35*, 155.
(14) Janssen, N. M. H.; Nieuwenhuys, B. E.; Ikai, M.; Tanaka, K.; Cholach, A. R. *Surf. Sci*. **1994**, *319*, L29.
(15) Cobden, P. D.; Janssen, N. M. H.; Van Breugel, Y.; Nieuwenhuys, B. E. *Surf. Sci*. **1996**, *366*, 432.
(16) Siera, J.; Cobden, P.; Tanaka, K.; Nieuwenhuys, B. E. *Catal. Lett*. **1991**, *10*, 335.
(17) Cobden, P. D.; Siera, J.; Nieuwenhuys, B. E. *J. Vac. Sci. Technol. A* **1992**, *10*, 2487.
(18) Slinko, M. M.; Fink, T.; Loher, T.; Maddens, H. H.; Lombardo, S. J.; Imbihl, R.; Ertl, G. *Surf. Sci*. **1992**, *264*, 157.
(19) Lombardo, S. J.; Fink, T.; Imbihl, R. *J. Chem. Phys*. **1993**, *98*, 5526.
(20) Thomas, G. E.; Weinberg, W. H. *Phys. Rev. Lett*. **1978**, *41*, 1181.
(21) Thiel, P. A.; Weinberg, W. H.; Yates, J. T., Jr. *Chem. Phys. Lett*. **1979**, *67*, 403.
(22) Umbach, E.; Kulkarni, S.; Feulner, P.; Menzel, D. *Surf. Sci*. **1979**, *88*, 65.
(23) Feulner, P.; Kulkarni, S.; Umbach, E.; Menzel, D. *Surf. Sci*. **1980**, *99*, 489.
(24) Hayden, B. E.; Kretzschmar, K.; Bradshaw, A. M. *Surf. Sci*. **1983**, *125*, 366.
(25) Conrad, H.; Scala, R.; Stenzel, W.; Unwin, R. *Surf. Sci*. **1984**, *145*, 1.
(26) Jakob, P.; Stichler, M.; Menzel, D. *Surf. Sci*. **1997**, *370*, L185.
(27) Stichler, M.; Menzel, D. *Surf. Sci*. **1997**, *391*, 47.
(28) Feulner, P.; Menzel, D. *Surf. Sci*. **1985**, *154*, 465.
(29) Yates Jr., J. T.; Peden, C. H. F.; Houston, J. E.; Goodman, D. W. *Surf. Sci*. **1985**, *160*, 37.
(30) Hofman, P.; Menzel, D. *Surf. Sci*. **1985**, *152/153*, 382.
(31) Feulner, P.; Pfnür, H.; Hofmann, P.; Menzel, D. *Surf. Sci*. **1986**, *173*, L576.
(32) Chou, M. Y.; Chelikowsky, J. R. *Phys. Rev. Lett*. **1987**, *59*, 1737.
(33) Lindroos, M.; Pfnür, H.; Menzel, D. *Surf. Sci*. **1987**, *192*, 421.
(34) Chou, M. Y.; Chelikowsky, J. R. *Phys. Rev. B* **1989**, *39*, 5623.
(35) Thiel, P. A.; Weinberg, W. H. *J. Chem. Phys*. **1980**, *73*, 4081.
(36) Nishida, T.; Egawa, C.; Naito, S.; Tamura, K. *J. Chem. Soc., Faraday Trans. 1* **1984**, *80*, 1567.
(37) Pfnür, H.; Held, G.; Lindroos, M.; Menzel, D. *Surf. Sci*. **1989**, *220*, 43.
(38) Thiel, P. A.; Weinberg, W. H.; Yates, J. T., Jr. *J. Chem. Phys*. **1979**, *71*, 1643.
(39) Seets, D. C.; Wheeler, M. C.; Mullins, C. B. *J. Chem. Phys*. **1995**, *103*, 10399.
(40) Koch, M. H.; Jakob, P.; Menzel, D. *Surf. Sci*. **1996**, *367*, 293.
(41) Held, G.; Menzel, D. *Surf. Sci*. **1995**, *327*, 301.
(42) Shi, S. K.; Schreifels, J. A.; White, J. M. *Surf. Sci*. **1981**, *105*, 1.
(43) Li, S. Y.; Rodriguez, J. A.; Hrbek, J. *J. Vac. Sci. Technol. A* **1997**, *15*, 1692.
(44) De Wolf, C. A.; Bakker, J. W.; Wouda, P. T.; Nieuwenhuys, B. E.; Baraldi, A.; Lizzit, S.; Kiskinova, M. To be published.